HHS Public Access

Author manuscript

Cell Metab. Author manuscript; available in PMC 2018 March 07.

Published in final edited form as:

Cell Metab. 2017 March 07; 25(3): 635–646. doi:10.1016/j.cmet.2017.02.007.

Orai1-mediated antimicrobial secretion from pancreatic acini shapes the gut microbiome and regulates gut innate immunity

Malini Ahuja[1,8], **Daniella M Schwartz**[2,8], **Mayank Tandon**[1], **Aran Son**[1], **Mei Zeng**[1], **William Swaim**[1], **Michael Eckhaus**[5], **Victoria Hoffman**[5], **Yiyuan Cui**[6], **Bo Xiao**[6], **Paul F Worley**[7], and **Shmuel Muallem**[1,9]

[1]National Institute of Dental and Craniofacial Research, National Institute of Health, Bethesda MD 20892

[2]National Institute of Arthritis & Musculoskeletal and Skin Diseases, National Institute of Health, Bethesda MD 20892

[5]Office of Research Services, National Institute of Health, Bethesda MD 20892

[6]Department of Neuroscience, Sichuan University, Chengdu 610041, China

[7]Department of Neuroscience, Johns Hopkins University, Baltimore, MD 21205

Abstract

The gut microbiome participates in numerous physiologic functions and communicates intimately with the host immune system. Antimicrobial peptides are critical components of intestinal innate immunity. We report a prominent role for antimicrobials secreted by pancreatic acinari in shaping the gut microbiome that is essential for intestinal innate immunity, barrier function, and survival. Deletion of the Ca^{2+} channel Orai1 in pancreatic acini of adult mice resulted in 60–70% mortality within three weeks. Despite robust activation of the intestinal innate immune response, mice lacking acinar Orai1 exhibited intestinal bacterial outgrowth and dysbiosis, ultimately causing systemic translocation, inflammation, and death. While digestive enzyme supplementation was ineffective, treatments constraining bacterial outgrowth (purified liquid diet, broad-spectrum antibiotics), rescued survival, feeding, and weight gain. Pancreatic levels of cathelicidin-related antimicrobial peptide (CRAMP) were reduced, and supplement of synthetic CRAMP prevented intestinal disease. These findings reveal a critical role for antimicrobial pancreatic secretion in gut innate immunity.

eTOC

[9]correspondence to and lead contact Shmuel.muallem@nih.gov.
[8]co-first authors

Authors contributions: MA, DMS, AS, MZ, WS performed experiments, ME, VH performed the pathological analysis in table S1, YC, BX, PFW generated the Orai1$^{fl/fl}$ mice, DMS and MT did the bioinformatics analysis, MA, DMS and SM conceived and directed the studies, SM wrote the manuscript with input from all authors.

While gut innate immunity is thought to be primarily maintained by intestinal epithelial cells, Ahuja et al. show that secretion of antimicrobials from pancreatic acinar cells regulates gut microbiota composition and innate immunity. Blocking acinar cell exocytosis in mice leads to gut dysbiosis, inflammation, systemic bacterial translocation and ultimately death.

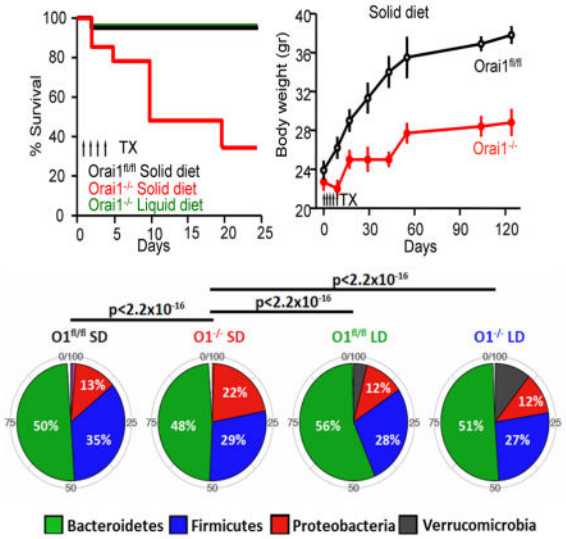

Introduction

The intestinal microbiome plays important roles in multiple physiological processes (Albenberg and Wu, 2014); dysbiosis is associated with infection and chronic inflammatory disorders (Salzman and Bevins, 2013). The intestine secretes antimicrobials; these directly shape the microbiome (Hooper, 2015) and recruit immune cells to further control the microbiota (Biragyn et al., 2002). Paneth and other intestinal cells secrete most antibacterial peptides (Clevers and Bevins, 2013), but other organs also secrete antibacterials into the intestine. Prominent among them is the pancreas, which in humans secretes 1–1.5 liters/day of juice into the intestine (Lee et al., 2012). The importance and role of pancreatic secretion in gut microbiota homeostasis is unknown.

The exocrine pancreas secretes digestive enzymes by exocytosis (Messenger et al., 2014). The pancreas also secretes antimicrobial proteins that consist about 10% of the proteins in the pancreatic juice (Medveczky et al., 2009). Exocytosis is stimulated primarily by receptor-evoked cytoplasmic Ca^{2+} ($[Ca^{2+}]_i$) increase. The Ca^{2+} signal entails repeated cycles of Ca^{2+} release from the ER followed by activation of store operated Ca^{2+} influx channels (SOCs) and pump-mediated Ca^{2+} extrusion to generate $[Ca^{2+}]_i$ oscillations (Cao et al., 2015). SOCs-mediated Ca^{2+} influx sustains the Ca^{2+} oscillations by refilling the ER. The primary components of the SOCs are the ER Ca^{2+} sensor STIM1 and the pore forming Orai1 (Hogan, 2015). Orai1 inhibitors are suggested as a promising approach to treat pancreatitis (Wen et al., 2015), a disease with no available treatment. However, considering the role of Orai1 in all Ca^{2+}-dependent cell functions, (Lacruz and Feske, 2015), such inhibition may be unsafe.

While evaluating the role of Orai1 in acinar cell function and survival, we discovered a prominent role of Orai1 and acinar cell exocytosis in shaping the microbiome that is essential for gut innate immunity. Deletion of Orai1 in pancreatic acinar cells of adult mice maintained on solid diet resulted in high mortality as a result of severe intestinal bacterial outgrowth with dysbiosis. Remarkably, death occurred in spite of an intact and fully activated intestinal innate immune response. Gut dysbiosis and survival was due to absent antimicrobial secretion by acinar cells and could be reversed by supplementing the gut with CRAMP peptide, and other measures that prevented bacterial overgrowth.

Results

Deletion of pancreatic acinar cells Orai1 results in death

The exocrine pancreas secretes digestive enzymes and a host of bacteriostatic peptides into the pancreatic juice that flows into the upper intestine. The role of pancreatic secretion in controlling the gut microbiota and barrier function has not been examined. Since pancreatic secretion is mediated by changes in $[Ca^{2+}]_i$, we addressed this question by generating a mouse model with targeted and inducible deletion of the store-operated Ca^{2+} channel (SOC) Orai1. Supplementary figure 1a–b(Figure S1a, b) shows the strategy for generating the $Orai1^{fl/fl}$ mice. Tamoxifen inducible Cre (CreER) controlled by the Elastase promoter was used to specifically delete Orai1 in pancreatic acinar cells (Ji et al., 2008). Figures S1c–g show specific deletion of Orai1 in pancreatic acini, while expression in multiple other tissues, the pancreatic duct, and blood vessels remains unaltered. Deletion of Orai1 did not affect polarity of the acinar structure, as indicated by normal expression of ZO1, IP_3 receptors (Figure S1h–k) and actin at the terminal web and granules at the apical pole stained with Rab27 and amylase (Figure S2).

Figure 1a shows that deletion of Orai1 in pancreatic acini of adult mice resulted in the death of 65% of mice on standard solid diet (SD) within three weeks. The mortality was unexpected since it was not seen in mice with embryonic T-cell Orai1 deletion (Hogan et al., 2010), mice with germline deletion of Orai1 by gene trap (Davis et al., 2015), or mice with conventional germline deletion of Orai1 (Gwack et al., 2008) that are partially rescued by outbreeding and delayed weaning. To test if deletion of Orai1 resulted in death from pancreatic insufficiency, digestive enzyme supplements were given in solid food or drinking water. Neither rescued the mice (Fig. 1b).

Necropsy of mice with $Orai1^{-/-}$ in pancreatic acini (henceforth referred to as $Orai1^{-/-}$ mice) and their $Orai1^{fl/fl}$ littermates revealed that $Orai1^{-/-}$ mice on SD were lean with reduced ingesta and had a high prevalence of gastrointestinal inflammation and systemic bacterial infection (supplementary table 1). We hypothesized that the $Orai1^{-/-}$ mice might be dying from gastrointestinal inflammation. Since human patients with gastrointestinal inflammation are treated with liquid diet (Sarbagili-Shabat et al., 2015), we maintained the $Orai1^{-/-}$ mice on a purified liquid diet (PLD). PLD had identical caloric, protein, lipid, carbohydrate, and fiber content to the standard SD but was derived from different dietary sources, including differences in the concentrations of specific amino acids (i.e. glutamate), carbohydrates (i.e. disaccharides), fatty acids (i.e. saturated, monounsaturated), and micronutrients (i.e. iron). Figure 1a shows that PLD completely rescued the $Orai1^{-/-}$ mice. Rescue by PLD further

supports the notion that impaired digestive enzyme secretion is not the cause of Orai1$^{-/-}$ mouse death.

The lack of ingesta and visceral fat suggested that the Orai1$^{-/-}$ mice do not eat normally, so their dietary intake was monitored. Application of Tamoxifen by gavage reduced eating by Orai1$^{fl/fl}$ and Orai1$^{-/-}$ mice (Figures 1c and 1d) for 2–3 days, but Orai1$^{-/-}$ mice on SD continued to consume less food (Figure 1c). This was not due to inhibition of feeding control: levels of the satiety hormones PYY, Leptin, Insulin, and Glucagon were all significantly reduced in Orai1$^{-/-}$ mice (Figure S3), indicating hunger. While pancreatic damage may have contributed to insulin and glucagon reduction, it would not have affected PYY and leptin levels. In addition, Orai1$^{-/-}$ mice on PLD resumed food consumption similar to Orai1$^{fl/fl}$ mice with a one-day delay (Figure 1d). We followed the body weight of eight surviving Orai1$^{-/-}$ mice on SD for 18 weeks. Figure 1e shows that these mice had very modest and slow weight gain. By contrast, Orai1$^{-/-}$ mice on PLD gained weight normally for the first 7 weeks, and then showed a significant but modest reduction (Figure 1f).

Deletion of Orai1 inhibits Ca^{2+} signaling, protein synthesis and exocytosis

Rescue of the Orai1$^{-/-}$ mice by PLD allowed us to determine the roles of Orai1 in Ca^{2+} signaling, digestive enzyme synthesis and exocytosis. Figures 2a–f show that deletion of Orai1 reduced Ca^{2+} release by about 50% and Ca^{2+} influx by about 80%. The reduction of Ca^{2+} release was due to reduced ER Ca^{2+} content, as evident from the reduced Ca^{2+} release by the SERCA inhibitor cyclopiazonic acid (CPA). Further, Figures 2d, e, g show that deletion of Orai1 reduced the frequency of Ca^{2+} oscillations evoked by 2 pM CCK.

Figure S2a shows that secretory granules remained clustered at the apical pole of Orai1$^{-/-}$ acinar cells. Measuring enzyme activity to obtain quantitative evaluation of digestive enzyme levels shows no marked difference in the level of the granule markers VAMP8 and Syntaxin 3 (Figure 2f), and Figure S2 shows similar staining of the granule marker Rab27 in Orai1$^{fl/fl}$ and Orai1$^{-/-}$ acinar cells, suggesting that deletion of Orai1 does not reduce the number of granules. However, lipase (Figure 2i), amylase (Figure 2j), and trypsin (Figure 2k) showed >50% reduction in hydrolytic activity. Moreover, the initial burst and sustained exocytosis were reduced by 80% in the Orai1$^{-/-}$ mice tested 10–112 days after deletion of Orai1 (Figure 2l). Hence, after accounting for the reduced total activity, exocytosis by the Orai1$^{-/-}$ pancreas is reduced by close to 90%. Fecal chymotrypsin level is a measure of pancreatic insufficiency *in vivo* (Lerch et al., 2010), was markedly reduced in feces of Orai1$^{-/-}$ mice maintained on either SD or PLD.

Deletion of Orai1 causes modest pancreatic damage

Although acinar polarity and tight junctions were not affected by deletion of Orai1 (Figures S1, S2), permeability of acinar tight junctions was damaged as indicated by mislocalization of the tight junction Na^{+} channel claudin-2 (Weber et al., 2015). Figures S4a–c show that Claudin-2 was absent from 60% of Orai1$^{-/-}$ acini, and that expression was diffuse when present. As a control, Claudin-2 expression in the Orai1$^{-/-}$ pancreatic duct was normal. Yet, analysis of edema spaces by H&E staining (Kim et al., 2009) (Figure S4d), staining for fat deposits and collagen (Lerch and Gorelick, 2013) (Figures S4d, and S4e) and measurement

of serum amylase (Figure S4g) and serum lipase (Figure S4h) revealed only modest pancreatic damage. Pancreatic damage can cause local and systemic inflammation (Lerch and Gorelick, 2013). We found mild leukocyte infiltration, predominantly of neutrophils, in the pancreas of Orai1$^{-/-}$ mice on SD (Figure S4i). Pancreatic MPO was also elevated (Figure 3a), in accordance with neutrophilic infiltration. By contrast, multiple serum inflammatory mediators were elevated in Orai1$^{-/-}$ mice on SD, but not Orai1$^{-/-}$ mice on PLD (Figures 3b–g). This was out of proportion to the mild pancreatic damage seen in Orai1$^{-/-}$ mice.

Deletion of Orai1 causes intestinal bacterial overgrowth and systemic infection

The gastrointestinal inflammation and bacterial infection noted in the pathological analysis led us to measure the intestinal bacterial burden in Orai1$^{-/-}$ mice.16S rRNA sequencing in Figure 4a showed increased cecal bacterial load in Orai1$^{-/-}$ mice on SD. Further, Figures 4b–d and S5a show abundant colonization of the duodenum, jejunum and the colonic mucosa of Orai1$^{-/-}$ mice on SD, but not on PLD, with both gram negative and positive bacteria. These bacteria were adherent to the mucosa, which was washed of non-adherent bacteria prior to fixation. Finally, scoring of duodena histological images (Figure 4e–g) revealed intestinal inflammation in the Orai1$^{-/-}$ mice on SD that was significantly reduced in mice fed PLD (Figure 4h). Notably, intestinal permeability was markedly increased in the Orai1$^{-/-}$ mice (Figure 4l), and the spleen, liver and the pancreas were infected with bacteria (Figure 4i–k), demonstrating bacterial translocation from the gut.

To investigate the protective mechanism of feeding Orai1$^{-/-}$ mice PLD, we measured the levels of fecal short chain free fatty acids (SCFAs). SCFAs are anti-inflammatory metabolites produced by gut bacteria, that also promote epithelial integrity (Thorburn et al., 2014). Figure 3h–k shows that Orai1$^{fl/fl}$ mice on PLD had increased concentrations of the SCFAs fecal acetate, propionate, and butyrate. Orai1$^{-/-}$ mice on PLD showed a similar trend, although it did reach statistical significance. Increased intestinal SCFAs in mice maintained on PLD may therefore partly explain the rescue of Orai1$^{-/-}$ mice by PLD. Of note, Orai1$^{-/-}$ mice on SD had high concentrations of all fecal SCFAs (Figure 3h–k). However, this is likely because these mice had bacterial overgrowth, which itself increases SCFA (Ou et al., 2013) and is a confounding factor not seen in the other groups.

Gut innate immunity is intact in Orai1$^{-/-}$ mice

Intestinal bacterial outgrowth raised the question of whether intestinal innate immunity is functional in Orai1$^{-/-}$ mice. Paneth cells are the primary secretors of intestinal antibacterials (Clevers and Bevins, 2013). Other intestinal epithelial cells secrete lectins like RegIIIγ, which promote the spatial segregation of microbiota and host cell surface in the intestine (Vaishnava et al., 2011). Figure 5a shows normal distribution and appearance of Paneth cells in the Orai1$^{fl/fl}$ intestine. Interestingly, deletion of Orai1 causes Paneth cell hyperplasia that is more prominent in mice on SD (Figure 5a–c, e–g). In addition, the granules in Paneth cells of Orai1$^{-/-}$ mice appear larger than the granules in Paneth cells of Orai1$^{fl/fl}$ mice, with most dramatic size differences in mice maintained on SD (insets in Figure 5a–c). Similar Paneth cell hyperplasia is observed in colitis (Puiman et al., 2011). Paneth cells store and secrete the bacterial lytic lysozyme that has a prominent role in intestinal innate immunity

(Hooper, 2015). Figures 5e–h show higher number of Paneth cells with lysozyme and higher level of lysozyme in Paneth cells from Orai1$^{-/-}$ mice. Staining for RegIIIγ reveals much higher levels in the intestines of Orai1$^{-/-}$ mice on SD (Figure 5i–l). Intestinal defensins and lectins recruit and activate immune cells like CD3+ T cells and IgA-producing B cells. The number of CD3+ cells is higher in the intestine of Orai1$^{-/-}$ mice fed SD (Figure 5m–p), as is the amount of intestinal IgA (Figure 5q–t). Bacterial burden (Figure 4b), RegIIIγ and IgA levels (Figure 5) in the intestine of Orai1$^{-/-}$ mice on PLD are significantly lower than that in Orai1$^{fl/fl}$ mice on SD. This may relate to differences in nutrient/fiber source that are known to affect intestinal immunity and microbiota (Ooi et al., 2014). Finally, the antibacterial activity of duodenal secretion is unaffected by deletion of pancreatic Orai1, indicating that Paneth cell antimicrobial peptides remain functional (Figure 5u). Together, the results in Figure 5 show that the intestinal epithelial innate immune response is intact and potently activated in Orai1$^{-/-}$ mice on SD.

A contributor to increased bacterial burden can be slow food transit time in the GI (Tursi, 2001). This was not the case with the Orai1$^{-/-}$ mice. Transit time of solid food was only slightly slower in mice maintained on SD (Figure S5b). Interestingly, transit time of liquid food was faster in Orai1$^{-/-}$ mice maintained on SD (Figure S5c), perhaps reflecting inflammation-related hypermotility, a phenomenon observed in patients with gastrointestinal infection (Navaneethan and Giannella, 2011).

Markedly impaired pancreatic antimicrobial activity is responsible for death in Orai1$^{-/-}$ mice

We hypothesized that the pancreatic antimicrobials are the missing component that is needed to control the microbiome. If so, then pancreas with Orai1$^{-/-}$ acini should have reduced antibacterial secretion. The cathelicidin-related peptide CRAMP is a major antimicrobial secreted by the pancreas. Figure 6a shows that total level of CRAMP is highly reduced in Orai1$^{-/-}$ pancreatic acini. To evaluate antimicrobial secretion, isolated pancreatic acini were stimulated for 30 min with 100 pM CCK. The secreted exudates were collected, concentrated and tested for their effect on *E. coli* growth. Figure 6c shows that exudate secreted by Orai1$^{fl/fl}$ pancreatic acini dose-dependently inhibited bacterial growth. By contrast, exudate secreted by Orai1$^{-/-}$ pancreatic acini of mice maintained on SD or PLD failed to prevent bacterial growth.

Interestingly, food consumption (Figure S5f) and survival (Figure 6e) of Orai1$^{-/-}$ mice on SD were rescued by treating the mice with broad-spectrum antibiotics prior to deletion of Orai1 to eradicate the gut bacteria (Figure 6d). To provide direct and strong evidence that the lack of antibacterials is the cause of the inflammation and death, we tested the effect of providing the gut with CRAMP peptide LL-37 that retains full antibacterial activity (Xhindoli et al., 2016). Most notably, Figure 6f shows that gavage with CRAMP LL-37, but not of scrambled 37-residue peptide, was sufficient to rescue the Orai1$^{-/-}$ mice on SD. As a final test, we performed microbiome transfer by gavaging Orai1$^{fl/fl}$ and Orai1$^{-/-}$ mice on PLD with cecal bacteria from Orai1$^{-/-}$ mice on SD. Figure 6g shows that transplant of cecal bacteria from Orai1$^{-/-}$ mice on SD to Orai1$^{-/-}$ mice on PLD resulted in death. As controls,

survival was intact in Orai1$^{-/-}$ mice on PLD transplanted with cecal material from Orai1$^{fl/fl}$ mice and Orai1$^{fl/fl}$ mice transplanted with cecal material from Orai1$^{-/-}$ mice on SD.

Lack of pancreatic antimicrobials disrupts the gut microbiome homeostasis

The results in Figure 6 indicate that reduced antibacterial activity indeed caused intestinal bacterial overgrowth, and that bacterial outgrowth is the cause of death in Orai1$^{-/-}$ mice on SD. We therefore compared the microbiome in Orai1$^{fl/fl}$ mice with Orai1$^{-/-}$ mice maintained on SD and PLD. We performed principal coordinate analysis (PCoA) based on unifrac phylogenetic distances, to probe the degree of similarity between the four different groups of intestinal microbiota. As seen in Figure 7a, the microbiome of Orai1$^{-/-}$ mice maintained on SD was significantly different from those of the other groups. This is evident as a significant shift along principal component 2. Remarkably, PLD shifts the microbiota of Orai1$^{-/-}$ mice towards that of Orai1$^{f/f}$ mice. The effect of diet and genotype on unifrac distances is statistically significant for both diet and genotype alone, as well as the interaction between the two ($p < 0.05$ for all cases).

We next compared the 5 most abundant phyla in each group of mice to probe for shifts in composition that might explain the differences between the microbiota of Orai1$^{-/-}$ mice maintained on SD and the other groups (Figure 7b). Strikingly, the Orai1$^{-/-}$ mice maintained on SD had a 2-fold higher abundance of proteobacteria than all other groups examined ($p<2e-16$, Fisher's exact t-test). Proteobacteria are considered pathogenic species that promote intestinal inflammation (Shin et al., 2015), indicating profound dysbiosis in the Orai1$^{-/-}$ mice maintained on SD. In order to identify the specific bacterial operational taxonomical units (OTUs) contributing to the shifting microbial pattern, we performed differential expression analysis. The results in Figure 7c indicate profound differences between the Orai1$^{-/-}$ and Orai1$^{f/f}$ mice, with enrichment in the Orai1$^{-/-}$ samples for inflammation-associated strains. We found 10 OTUs with significantly (FDR-corrected $p<0.05$) higher expression in the Orai1$^{-/-}$ mice maintained on SD, and 8 OTUs with significantly higher expression in the Orai1$^{fl/fl}$ mice. Several inflammation-associated strains, including *Succinivibrionaceae* species, *Enterobacter* species, and *Prevotella* species (Loh and Blaut, 2012), were increased in Orai1$^{-/-}$ mice (Figure 7d–f). Maintaining mice on a PLD shifted abundance of OTUs towards levels seen in Orai1$^{fl/fl}$ mice. Taken together, these results lead us to conclude that acute pancreatic deletion of Orai1$^{-/-}$ causes pathologic alterations in microbiome composition and diversity that drive intestinal inflammation and ultimately lead to bacterial translocation, systemic inflammation, and death.

Discussion

The central findings of the present work are that pancreatic acinar cell secretion plays a crucial role in controlling the microbiome and gut innate immunity, and that disrupting this pancreatic function leads to gut inflammation and death. The general belief is that gut innate immunity is maitained primarily by intestinal cells, in particular Paneth cells, which secrete antimicrobials with the capacity to recruit and activate immune cells. However, compromised intestinal cell immunity does not appear to be a major contributor to the altered microbiome of Orai1$^{-/-}$ mice, which exhibited Paneth cell hyperplasia, secretion of

intestinal-derived antimicrobials, and activation of intestinal immune cells (Figure 5). Instead, pancreatic synthesis and secretion of antimicrobials was markedly inhibited (Figure 6).

Pancreatic secretion maintains mucosal barrier integrity through maintenance of intestinal integrity and control of the microbiome. Pancreatic antibacterial secretion controls bacterial outgrowth, favors beneficial species, and limits pathogenic species (Figures 7). Bacterial overgrowth and dysbiosis led to intestinal inflammation, which likely resulted in systemic infection. Pancreatic secretion also maintains barrier integrity: increased intestinal permeability is observed in acute pancreatitis and other pancreatic diseases (Leal-Lopes et al., 2015). This may underlie the increased intestinal permeability in Orai1$^{-/-}$ mice. However, increased intestinal permeability is not sufficient to cause systemic inflammation and death, as the Orai1$^{-/-}$ mice on liquid diet did not develop these manifestations unless they were transplanted with pathogenic microbiota (Figures 6, 7). Future studies using proteomic analysis combined with targeted deletion of specific pancreatic antimicrobials may identify the key effectors of pancreatic-mediated intestinal immunity.

Pancreatic secretion is largely $[Ca^{2+}]_i$-mediated, and Ca^{2+} influx through Orai1 is central to receptor-evoked Ca^{2+} signaling (Figure 2). Deletion of Orai1 markedly reduced Ca^{2+} influx, frequency of Ca^{2+} oscillations, and digestive enzyme exocytosis. Reduction in digestive enzyme content was unexpected (Figure 2i–k, m), as secretory granules appeared normal (Figures 2h and S2b). This may be the result of reduced ER Ca^{2+} content in Orai1$^{-/-}$ cells (Figure 2), since ER Ca^{2+} is required for protein synthesis (Sans et al., 2002). However, reduced digestive enzymes did not cause death in Orai1$^{-/-}$ mice maintained on solid diet, since the mice were rescued by purified nonelemental liquid diet, by antibiotic sterilization, and by CRAMP gavage (Figure 6e, f), but not by digestive enzyme supplementation (Figure 1a, b).

The human pancreas secretes 1–1.5 liters/day of juice into the intestine that contains antimicrobials and digestive enzymes. However, digestive enzymes do not have antibacterial activity (Rubinstein et al., 1985) and digestive enzyme supplementation could not rescue the mice (Fig. 1b). Because deletion of Orai1 inhibits synthesis and secretion of antimicrobials (Figure 6a–c), our findings also indicate that pancreatic antibacterial secretion is stimulated by GPCR-evoked Ca^{2+} signaling that requires Orai1-mediated Ca^{2+} influx. Moreover, the present findings emphasize the importance of diet in modulating the microbiome. Effects of diet on the microbiome is well established and liquid diets are used as first-line therapy in Crohn's disease (Day and Burgess, 2013). The advantages of the liquid diet are reduced allergenic load, anti-inflammatory action, and restoration of intestinal barrier (Ruemmele et al., 2014). We confirmed these findings by showing that liquid diet increases the fecal levels of SCFAs that are associated with reduced inflammation. The present findings suggest that an additional major benefit of the liquid diet is prevention of bacterial outgrowth and dysbiosis, which may enhance mucosal defense and therefore ameliorate the disease. Because liquid and solid diets are derived from different sources, they contain different concentrations of specific nutrients and micronutrients. This could underlie the alterations in SCFA content and contribute to to the rescue of Orai1$^{-/-}$ mice by liquid diet.

Orai1 function is essential for development and function of T cells and has a key role in immunity and inflammation (Shaw et al., 2013). Patients with ORAI1 mutations have a high rate of gastrointestinal infection and diarrhea, which may in part reflect decreased production of pancreatic antimicrobials (McCarl et al., 2009). Although fatal spontaneous colitis has not been described in mice with germline deletion of Orai1, these mice have deleterious phenotypes with high perinatal lethality requiring specialized housing conditions, which could mask the development of gastrointestinal morbidity (Gwack et al., 2008; Vig et al., 2008). Inhibitors of Orai1 are being developed to control several Ca^{2+}-dependent diseases and inflammatory diseases, including several forms of acute pancreatitis (Wen et al., 2015). Our findings call for caution in the use of such inhibitors. In the case of acute pancreatitis, partial protection is achieved by inhibition of TRPC3, another receptor-activated Ca^{2+} influx channel (Hong et al., 2011; Kim et al., 2009). A more suitable approach may be the combined use of partial inhibition of Orai1 and of TRPC channels to treat inflammatory diseases, while maintaining the patient on liquid diet and monitoring for acute intestinal inflammation.

Our findings should have implications for exocrine pancreas-associated diseases. They suggest that pancreatic diseases associated with damage to acinar cells may be associated with dysbiosis of the intestinal microbiome. Indeed, high intestinal bacterial burden has been reported in cystic fibrosis patients with pancreatic insufficiency (Fridge et al., 2007) and in patients with severe acute pancreatitis (Tan et al., 2015). Our findings may also be relevant to patients undergoing pancreatectomy. Up to 80% of patients who undergo total pancreatectomy experience profound malnutrition, diarrhea, and steatorrhea (Shahbazov et al., 2016), which is not significantly affected by pancreatic enzyme replacement. Indeed, many patients many require specific enteral diets (Zakaria et al., 2016). The etiology of these symptoms in pancreatectomy patients is unclear; the present findings suggest that these features may be driven by intestinal dysbiosis secondary to absent antimicrobials.

The role of Orai1 and more broadly of pancreatic secretion in maintaining the microbiome may open novel avenues for the therapeutic development. Patients with pancreatitis can develop severe infection-related morbidity (Zerem, 2014); mortality often correlates with severity of pancreatitis, although the mechanism has been as yet unclear. Bacterial translocation secondary to intestinal inflammation may represent an important aspect of pancreatitis-related morbidity and should be explored further. Indeed, the use of antimicrobial peptides to alter intestinal microbiome composition may represent a novel therapeutic route for pancreatic disease-related morbidity and mortality.

Methods

Orai1 knockout mice

$Orai1^{fl/fl}$ mice (see extended methods) were bred with Tamoxifen inducible elastase promoter driven Cre transgenic mice (Ji et al., 2008). $Orai1^{fl/fl}$ were bred with $Orai1^{fl+/fl-}$/Cre and $Orai1^{fl/fl}$/Cre and were used to generate mice with Orai1 deleted in pancreatic acinar cells. $Orai1^{fl/f}$ littermates were used as WT controls. $Orai1^{fl/fl}$/Cre mice were injected or gavaged with 5mg/40g BW Tamoxifen in sunflower oil for 5 consecutive days. All the mice were on C57/BL6J background. Mice were always fed from the same

batch of diet, and Orai1f/f mice were cohoused with Orai1$^{-/-}$ mice and housed in the same facility.

Liquid and Solid Diets

The mice were fed AIN-76 purified liquid diet (PLD) or the white round pelleted solid food (SD) from Bioserv (SD: F0076, SD for pancreatic enzyme replacement: F0761, LPD: F1268SP). Feeding started 48 hrs prior to induction of Cre and continued until mouse euthanasia or spontaneous death. LPD suspended in water was administered in graduated glass tubes in steel holders. SD was administered in graduated glass tubes and holders from Bioserv. Graduated glass tubes were used to calculate food intake.

Treatment with CRAMP and scrambled peptides

For CRAMP peptide LL-37 and the scrambled peptide (Sun et al., 2015) gavage, Orai1$^{-/-}$ mice on SD were gavaged with 100μg in 200ul of PBS, 6 days before start of TX, 4 hours prior to the first two TX applications, on days 6, 7, 13 and 14 after start of TX. The mice were euthanized at day 21 and cecal contents were collected.

Cecal gavage

Orai1$^{-/-}$ mice fed CLD were treated with Neomycin (1g/L), Valinomycin (0.5g/L) and Primaxin (0.5g/L) in drinking water for 2 weeks. Cecal contents from donor mice were collected aseptically and diluted in 100μl of sterile PBS and kept at at −80ºC. Thawed samples were diluted 1:50 in sterile PBS and 150 μl were inoculate to Orai1$^{-/-}$ mice on PLD by gavage (Ellekilde et al., 2014).

Pancreatic and intestinal antibacterial secretion

Disperesed pancreatric acini were stimulated with 100pM CCK for 30 min at 37°C. The supernatants were collected by centrifugation at 1000xg for 5 min, supplemented with protease inhibitors cocktail tablet (Roche) and concentrated to 100 μl using 4K filters from Millipore. Finely minced duodena in solution A were stimulated with 100μM carbachol for 45 min at 37ºC. The supernatants were collected and concentrated as above. Anti-bacterial activity was evaluated against *E. coli* DH10B (Life Technologies) grown in LB broth to OD 0.2–0.3.

SCFA analysis

Fecal pellets were homogenized in 400 μL 30 mM HCl, isotopically-labeled acetate (0.125 mM), butyrate (0.125mM), and hexanoate (0.0125mM). 250 μL of Methyl tert-butyl ether (MTBE) was added, and the mixture was vortexed twice for 10 sec. Samples were centrifuged for 1 min and MTBE was transfered to auto-sampler vials. 10 μl of MTBE from each sample were pooled for quality control. Calibration standards were prepared along with the samples. GC-MS analysis was performed on an Agilent 69890N GC-5973 MS detector with the parameters given in extended methods. Data were processed using Mass Hunter Quantitative analysis version B.07.00. SCFAs were normalized to the nearest isotope labeled internal standard and quantitated using 2 replicated injections of 5 standards with accuracy better than 80% for each standard.

Analysis of cecal microbiome

Cecal contents were collected aseptically 5 days after the last TX gavage, before death of mice on SD. The GI tract was isolated by grabbing the colon with forceps, pulling out the GI tract, cutting and laying it on a surgical table lined with clean towels. The fecal material in the cecum was squeezed into a 2mL cryovial, snap frozen in liquid N_2, and stored at −80°C. DNA was extracted from thawed samples with QiaAMP Fast DNA Stool Mini kit (Qiagen) to analyze bacterial load and for microbiome analysis at UC Davis Host-Microbe Systems Biology Core by 16S gene variable regions. Sequences were processed by QIIME analysis pipeline for taxonomic classification and alpha and beta diversity.

Phylogenetic analyses of sequencing data

Read count data were exported as BIOM tables and analyzed and visualized using the ‘phyloseq’ package (version 1.14) distributed as part of the Bioconductor (version 2.30) (Huber et al., 2015) repository for the R statistical programming language (R version 3.2.2). Of the 33 samples sequenced, four were identified to be outliers based on the ROBPCA algorithm (Hubert et al., 2005) and were excluded from further analysis. For principal coordinates analysis, a minimum read count of 10 was applied before coordinate transformations, and statistical significance was calculated using adonis function in the ‘vegan‘ package (version 2.4-1). Top OTU abundances were computed as the sum of read counts across replicate animal samples in each condition.

Differential expression analysis of OTUs

After application of a filtering step, the raw counts were prepared for differential expression testing. The count data were analyzed for differential expression due to genotype in the SD condition using the DESeq2 package (version 1.12.4) (Love et al., 2014) where statistical significance was calculated based on the Wald test using the Benjamini-Hochberg correction for multiple comparisons.

Detailed methods for all procedures are described in the supplementary information

Supplementary Material

Refer to Web version on PubMed Central for supplementary material.

Acknowledgments

We thank Drs. Craig Logsdon (University of Texas, M.D. Anderson Cancer Center, Houston) and Baoan Ji (Mayo Clinic, Rochester) for providing the Cre mice, Dr. Owen G. Schwartz (Washington Hospital center) for help in reviewing and editing. This work was supported by intramural grant DE000735 to SM and NIH granny R01 DA010309 to PFW. The microbiome analysis was done by University of California Davis Mouse biology core and the SCFAs analysis was done by the Metabolomics at University of Michigan.

References

Albenberg LG, Wu GD. Diet and the intestinal microbiome: associations, functions, and implications for health and disease. Gastroenterology. 2014; 146:1564–1572. [PubMed: 24503132]

Biragyn A, Ruffini PA, Leifer CA, Klyushnenkova E, Shakhov A, Chertov O, Shirakawa AK, Farber JM, Segal DM, Oppenheim JJ, et al. Toll-like receptor 4-dependent activation of dendritic cells by beta-defensin 2. Science. 2002; 298:1025–1029. [PubMed: 12411706]

Cao X, Choi S, Maleth JJ, Park S, Ahuja M, Muallem S. The ER/PM microdomain, PI(4,5)P(2) and the regulation of STIM1-Orai1 channel function. Cell calcium. 2015; 58:342–348. [PubMed: 25843208]

Clevers HC, Bevins CL. Paneth cells: maestros of the small intestinal crypts. Annual review of physiology. 2013; 75:289–311.

Davis FM, Janoshazi A, Janardhan KS, Steinckwich N, D'Agostin DM, Petranka JG, Desai PN, Roberts-Thomson SJ, Bird GS, Tucker DK, et al. Essential role of Orai1 store-operated calcium channels in lactation. Proceedings of the National Academy of Sciences of the United States of America. 2015; 112:5827–5832. [PubMed: 25902527]

Day AS, Burgess L. Exclusive enteral nutrition and induction of remission of active Crohn's disease in children. Expert Rev Clin Immunol. 2013; 9:375–383. quiz 384. [PubMed: 23557272]

Ellekilde M, Selfjord E, Larsen CS, Jakesevic M, Rune I, Tranberg B, Vogensen FK, Nielsen DS, Bahl MI, Licht TR, et al. Transfer of gut microbiota from lean and obese mice to antibiotic-treated mice. Sci Rep. 2014; 4:5922. [PubMed: 25082483]

Fridge JL, Conrad C, Gerson L, Castillo RO, Cox K. Risk factors for small bowel bacterial overgrowth in cystic fibrosis. J Pediatr Gastroenterol Nutr. 2007; 44:212–218. [PubMed: 17255834]

Gwack Y, Srikanth S, Oh-Hora M, Hogan PG, Lamperti ED, Yamashita M, Gelinas C, Neems DS, Sasaki Y, Feske S, et al. Hair loss and defective T- and B-cell function in mice lacking ORAI1. Mol Cell Biol. 2008; 28:5209–5222. [PubMed: 18591248]

Hogan PG. The STIM1-ORAI1 microdomain. Cell calcium. 2015; 58:357–367. [PubMed: 26215475]

Hogan PG, Lewis RS, Rao A. Molecular basis of calcium signaling in lymphocytes: STIM and ORAI. Annu Rev Immunol. 2010; 28:491–533. [PubMed: 20307213]

Hong JH, Li Q, Kim MS, Shin DM, Feske S, Birnbaumer L, Cheng KT, Ambudkar IS, Muallem S. Polarized but differential localization and recruitment of STIM1, Orai1 and TRPC channels in secretory cells. Traffic. 2011; 12:232–245. [PubMed: 21054717]

Hooper LV. Epithelial cell contributions to intestinal immunity. Adv Immunol. 2015; 126:129–172. [PubMed: 25727289]

Huber W, Carey VJ, Gentleman R, Anders S, Carlson M, Carvalho BS, Bravo HC, Davis S, Gatto L, Girke T, et al. Orchestrating high-throughput genomic analysis with Bioconductor. Nat Methods. 2015; 12:115–121. [PubMed: 25633503]

Hubert M, Rousseeuw PJ, Vanden Branden K. ROBPCA: A new approach to robust principal component analysis. Technometrics. 2005; 47:64–79.

Ji B, Song J, Tsou L, Bi Y, Gaiser S, Mortensen R, Logsdon C. Robust acinar cell transgene expression of CreErT via BAC recombineering. Genesis. 2008; 46:390–395. [PubMed: 18693271]

Kim MS, Hong JH, Li Q, Shin DM, Abramowitz J, Birnbaumer L, Muallem S. Deletion of TRPC3 in mice reduces store-operated Ca2+ influx and the severity of acute pancreatitis. Gastroenterology. 2009; 137:1509–1517. [PubMed: 19622358]

Lacruz RS, Feske S. Diseases caused by mutations in ORAI1 and STIM1. Ann N Y Acad Sci. 2015; 1356:45–79. [PubMed: 26469693]

Leal-Lopes C, Velloso FJ, Campopiano JC, Sogayar MC, Correa RG. Roles of Commensal Microbiota in Pancreas Homeostasis and Pancreatic Pathologies. J Diabetes Res. 2015; 2015:284680. [PubMed: 26347203]

Lee MG, Ohana E, Park HW, Yang D, Muallem S. Molecular mechanism of pancreatic and salivary gland fluid and HCO3 secretion. Physiological reviews. 2012; 92:39–74. [PubMed: 22298651]

Lerch MM, Gorelick FS. Models of acute and chronic pancreatitis. Gastroenterology. 2013; 144:1180–1193. [PubMed: 23622127]

Lerch MM, Mayerle J, Aghdassi AA, Budde C, Nitsche C, Sauter G, Persike M, Gunther A, Simon P, Weiss FU. Advances in the etiology of chronic pancreatitis. Dig Dis. 2010; 28:324–329. [PubMed: 20814206]

Loh G, Blaut M. Role of commensal gut bacteria in inflammatory bowel diseases. Gut microbes. 2012; 3:544–555. [PubMed: 23060017]

Love MI, Huber W, Anders S. Moderated estimation of fold change and dispersion for RNA-seq data with DESeq2. Genome Biol. 2014; 15:550. [PubMed: 25516281]

McCarl CA, Picard C, Khalil S, Kawasaki T, Rother J, Papolos A, Kutok J, Hivroz C, Ledeist F, Plogmann K, et al. ORAI1 deficiency and lack of store-operated Ca2+ entry cause immunodeficiency, myopathy, and ectodermal dysplasia. J Allergy Clin Immunol. 2009; 124:1311–1318. e1317. [PubMed: 20004786]

Medveczky P, Szmola R, Sahin-Toth M. Proteolytic activation of human pancreatitis-associated protein is required for peptidoglycan binding and bacterial aggregation. Biochem J. 2009; 420:335–343. [PubMed: 19254208]

Messenger SW, Falkowski MA, Groblewski GE. Ca(2)(+)-regulated secretory granule exocytosis in pancreatic and parotid acinar cells. Cell calcium. 2014; 55:369–375. [PubMed: 24742357]

Navaneethan U, Giannella RA. Infectious colitis. Current opinion in gastroenterology. 2011; 27:66–71. [PubMed: 20856114]

Ooi JH, Waddell A, Lin YD, Albert I, Rust LT, Holden V, Cantorna MT. Dominant effects of the diet on the microbiome and the local and systemic immune response in mice. PLoS One. 2014; 9:e86366. [PubMed: 24489720]

Ou J, Carbonero F, Zoetendal EG, DeLany JP, Wang M, Newton K, Gaskins HR, O'Keefe SJ. Diet, microbiota, and microbial metabolites in colon cancer risk in rural Africans and African Americans. The American journal of clinical nutrition. 2013; 98:111–120. [PubMed: 23719549]

Puiman PJ, Burger-Van Paassen N, Schaart MW, De Bruijn AC, De Krijger RR, Tibboel D, Van Goudoever JB, Renes IB. Paneth cell hyperplasia and metaplasia in necrotizing enterocolitis. Pediatr Res. 2011; 69:217–223. [PubMed: 21372757]

Rubinstein E, Mark Z, Haspel J, Ben-Ari G, Dreznik Z, Mirelman D, Tadmor A. Antibacterial activity of the pancreatic fluid. Gastroenterology. 1985; 88:927–932. [PubMed: 3882511]

Ruemmele FM, Pigneur B, Garnier-Lengline H. Enteral nutrition as treatment option for Crohn's disease: in kids only? Nestle Nutr Inst Workshop Ser. 2014; 79:115–123. [PubMed: 25227299]

Salzman NH, Bevins CL. Dysbiosis--a consequence of Paneth cell dysfunction. Semin Immunol. 2013; 25:334–341. [PubMed: 24239045]

Sans MD, Kimball SR, Williams JA. Effect of CCK and intracellular calcium to regulate eIF2B and protein synthesis in rat pancreatic acinar cells. Am J Physiol Gastrointest Liver Physiol. 2002; 282:G267–276. [PubMed: 11804848]

Sarbagili-Shabat C, Sigall-Boneh R, Levine A. Nutritional therapy in inflammatory bowel disease. Current opinion in gastroenterology. 2015; 31:303–308. [PubMed: 25887458]

Shahbazov R, Yoshimatsu G, Haque WZ, Khan OS, Saracino G, Lawrence MC, Kim PT, Onaca N, Naziruddin B, Levy MF. Clinical effectiveness of a pylorus-preserving procedure on total pancreatectomy with islet autotransplantation. American journal of surgery. 2016

Shaw PJ, Qu B, Hoth M, Feske S. Molecular regulation of CRAC channels and their role in lymphocyte function. Cell Mol Life Sci. 2013; 70:2637–2656. [PubMed: 23052215]

Shin NR, Whon TW, Bae JW. Proteobacteria: microbial signature of dysbiosis in gut microbiota. Trends in biotechnology. 2015; 33:496–503. [PubMed: 26210164]

Sun J, Furio L, Mecheri R, van der Does AM, Lundeberg E, Saveanu L, Chen Y, van Endert P, Agerberth B, Diana J. Pancreatic beta-Cells Limit Autoimmune Diabetes via an Immunoregulatory Antimicrobial Peptide Expressed under the Influence of the Gut Microbiota. Immunity. 2015; 43:304–317. [PubMed: 26253786]

Tan C, Ling Z, Huang Y, Cao Y, Liu Q, Cai T, Yuan H, Liu C, Li Y, Xu K. Dysbiosis of Intestinal Microbiota Associated With Inflammation Involved in the Progression of Acute Pancreatitis. Pancreas. 2015; 44:868–875. [PubMed: 25931253]

Thorburn AN, Macia L, Mackay CR. Diet, metabolites, and "western-lifestyle" inflammatory diseases. Immunity. 2014; 40:833–842. [PubMed: 24950203]

Tursi A. Delayed orocecal transit time and bacterial overgrowth in Crohn's disease. J Clin Gastroenterol. 2001; 32:274–275. [PubMed: 11246364]

Vaishnava S, Yamamoto M, Severson KM, Ruhn KA, Yu X, Koren O, Ley R, Wakeland EK, Hooper LV. The antibacterial lectin RegIIIgamma promotes the spatial segregation of microbiota and host in the intestine. Science. 2011; 334:255–258. [PubMed: 21998396]

Vig M, DeHaven WI, Bird GS, Billingsley JM, Wang H, Rao PE, Hutchings AB, Jouvin MH, Putney JW, Kinet JP. Defective mast cell effector functions in mice lacking the CRACM1 pore subunit of store-operated calcium release-activated calcium channels. Nat Immunol. 2008; 9:89–96. [PubMed: 18059270]

Weber CR, Liang GH, Wang Y, Das S, Shen L, Yu AS, Nelson DJ, Turner JR. Claudin-2-dependent paracellular channels are dynamically gated. Elife. 2015; 4

Wen L, Voronina S, Javed MA, Awais M, Szatmary P, Latawiec D, Chvanov M, Collier D, Huang W, Barrett J, et al. Inhibitors of ORAI1 Prevent Cytosolic Calcium-Associated Injury of Human Pancreatic Acinar Cells and Acute Pancreatitis in 3 Mouse Models. Gastroenterology. 2015; 149:481–492. e487. [PubMed: 25917787]

Xhindoli D, Pacor S, Benincasa M, Scocchi M, Gennaro R, Tossi A. The human cathelicidin LL-37--A pore-forming antibacterial peptide and host-cell modulator. Biochimica et biophysica acta. 2016; 1858:546–566. [PubMed: 26556394]

Zakaria HM, Stauffer JA, Raimondo M, Woodward TA, Wallace MB, Asbun HJ. Total pancreatectomy: Short- and long-term outcomes at a high-volume pancreas center. World journal of gastrointestinal surgery. 2016; 8:634–642. [PubMed: 27721927]

Zerem E. Treatment of severe acute pancreatitis and its complications. World J Gastroenterol. 2014; 20:13879–13892. [PubMed: 25320523]

Highlights

- Orai1 controls pancreatic acinar cell antimicrobial secretion
- Deletion of acinar Orai1 in adult mice results in intestinal dysbiosis
- Dysbiosis causes systemic bacteremia and death
- Pancreatic antibacterial secretion is vital for the gut innate immunity

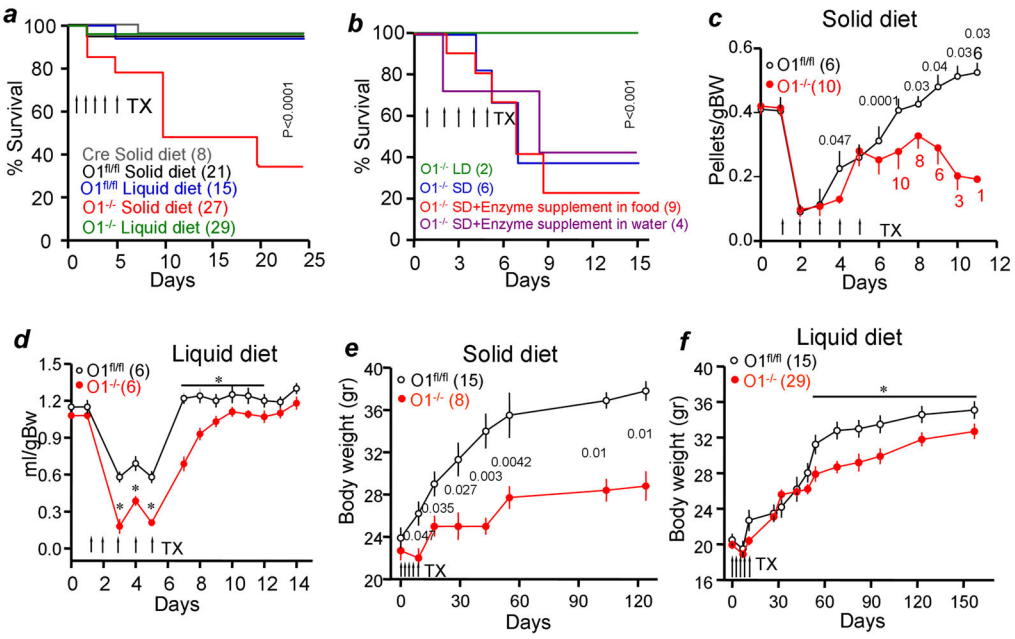

Figure 1. Deletion of pancreatic acinar cells Orai1 results in death

In all experiments, the number of mice in each experiment and condition are given in brackets and p values are listed next to the points.

(a) Mice carrying the pancreatic Cre, Orai1$^{fl/fl}$ and Orai1$^{-/-}$ mice were maintained on solid or liquid diets and survival determined. TX, tamoxifen

(b) Orai1$^{-/-}$ mice maintained on solid (SD) or liquid (LD) diets were supplemented with digestive enzymes in the SD (red) or drinking water (purple).

(c) Consumption of solid food by Orai1$^{fl/fl}$ and Orai1$^{-/-}$ mice.

(d) Consumption of liquid food by Orai1$^{fl/fl}$ and Orai1$^{-/-}$ mice. * denotes p<0.05 or better.

(e) Body weight of Orai1$^{fl/fl}$ and of surviving Orai1$^{-/-}$ mice maintained on solid diet.

(f) Body weight of Orai1$^{fl/fl}$ and Orai1$^{-/-}$ mice maintained on liquid diet. * denotes p<0.05 or better.

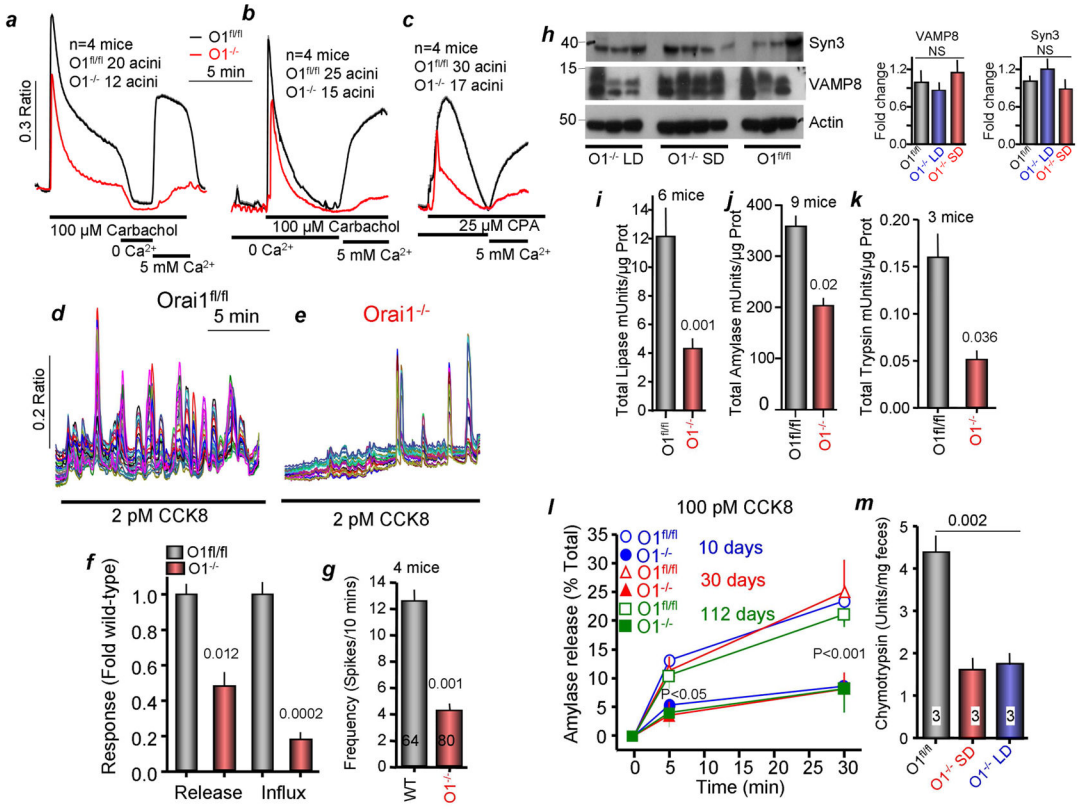

Figure 2. Effect of deletion of Orai1 on Ca^{2+} signaling, enzymes content and exocytosis

All experiments are with Orai1$^{fl/fl}$ mice maintained on solid diet (controls) and Orai1$^{-/-}$ mice maintained on liquid diet for 10 days after last gavage with Tamoxifen, except in (m).

(a) Ca^{2+} signaling evoked by carbachol stimulation in Orai1$^{fl/fl}$ (black trace) and Orai1$^{-/-}$ (red trace) acinar cells in Ca^{2+} containing medium. Where indicated the cells were exposed to 0 and 5 mM external Ca^{2+} to assay Ca^{2+} influx.

(b, c) Acinar cells in Ca^{2+}-free solution were stimulated with 100 μM carbachol (b) or 25 μM CPA (c) to assay Ca^{2+} release from stores and then exposed to 5 mM external Ca^{2+} to determine store-operated Ca^{2+} influx. Traces in (a–c) are mean±s.e.m of the number of acini obtained from 4 mice of each line. Each acinus comprised of 5–10 cells.

(d, e) Orai1$^{fl/fl}$ (d) and Orai1$^{-/-}$ acinar cells (e) were stimulated with 2 pM CCK8 to evaluate receptor-stimulated Ca^{2+} oscillations.

(f) Summary of Ca^{2+} release and influx. Here and in (g, i, k) the p values are listed in the columns.

(g) Summary of Ca^{2+} oscillation frequency recorded in 64 Orai1$^{fl/fl}$ and 80 Orai1$^{-/-}$ acinar cells.

(h) Protein levels of the granule markers syntaxin 3 and VAMP8, and of actin. The columns show the average staining intensity relative to actin and is plotted as mean±s.e.m.

(i–k) Activity of total lipase (i, 6 mice), amylase (j, 9 mice) and trypsin (k, 3 mice) in Orai1$^{fl/fl}$ (black) and Orai1$^{-/-}$ acinar cells (red).

(l) Time course of exocytosis stimulated by 100 pM CCK8 in acini obtained from age-matched Orai1$^{fl/fl}$ and Orai1$^{-/-}$ mice 10 (blue, circles), 30 (red, triangles) and 112 (green, squares) days after deletion of Orai1.

(m) Chymotrypsin in feces of Orai1$^{fl/fl}$ mice (black) and Orai1$^{-/-}$ mice maintained on solid (red) and liquid diets (blue) for 10 days after final Tamoxifen gavage.

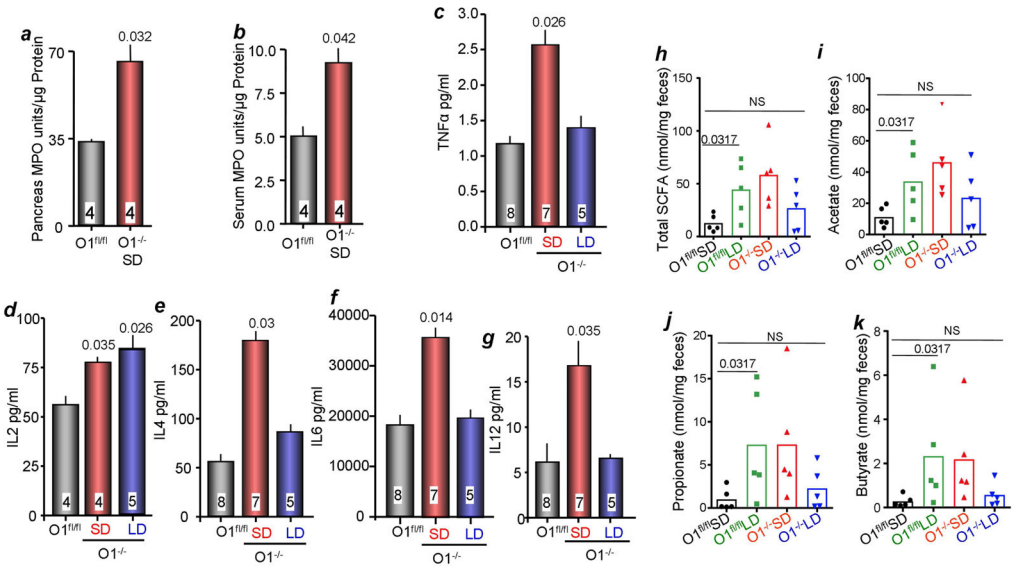

Figure 3. Inflammatory mediators and inflammatory in Orai1$^{fl/fl}$ and Orai1$^{-/-}$ mice the pancreas

(a) MPO was measured in extracts prepared from the pancreas of Orai1$^{fl/fl}$ (black) and Orai1$^{-/-}$ mice (red).

(b–g) Serum from Orai1$^{fl/fl}$ (black), Orai1$^{-/-}$ mice maintained on solid (red) and liquid diets (blue) was used to measure MPO (b), TNFα (c), IL2 (d), IL4 (e), IL6 (f), and IL12 (g). The number of mice is indicated in the column and the p values relative to the level in Orai1$^{fl/fl}$ are listed above the columns.

(h–k) Fecal SCFAs were analyzed in Orai1$^{fl/fl}$ maintained on solid (black) or liquid diet (green) and Orai1$^{-/-}$ mice maintained on liquid diet. Shown are the total level of SCFAs (h) and the levels of acetate (i), propionate (j) and butyrate (k).

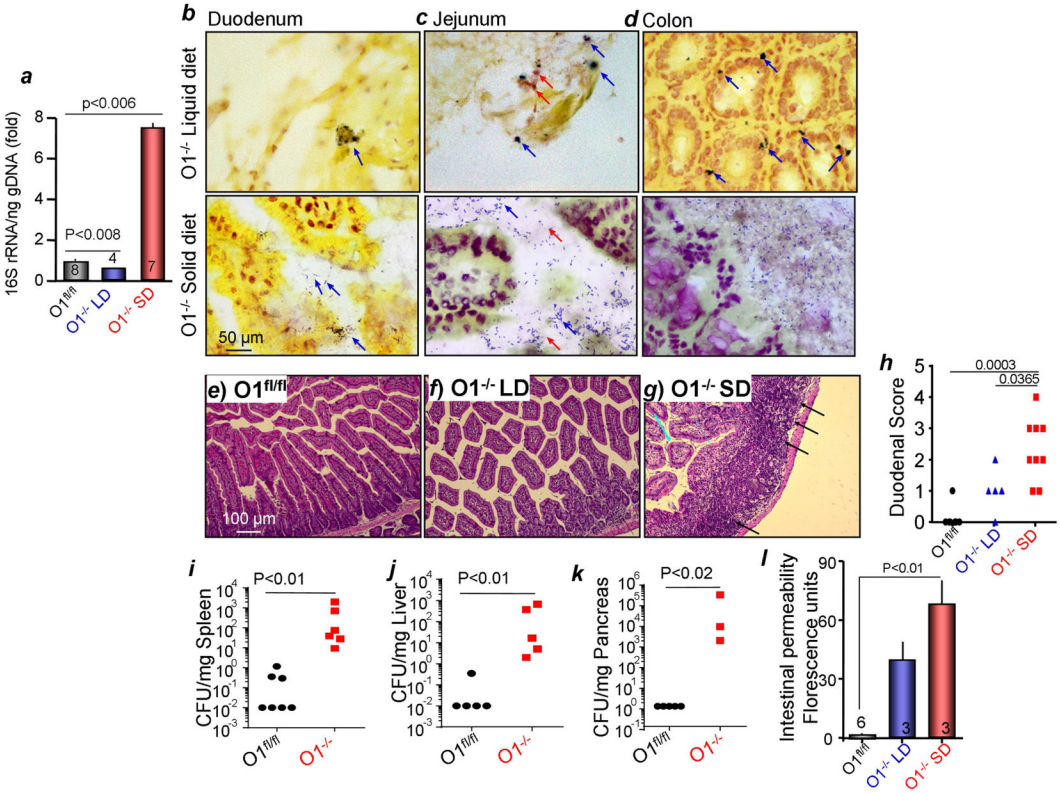

Figure 4. Bacterial burden and intestinal inflammation in Orai1$^{-/-}$ mice

(a) Cecal bacterial 16S rRNA was measured in Orai1$^{fl/fl}$ mice and Orai1$^{-/-}$ mice maintained on liquid (LD) or solid diets (SD).

(b–d) Duodenal (b), Jejunal (c) and colonic (d) sections obtained from Orai1$^{-/-}$ mice maintained on liquid (upper images) or solid diets (lower images) were stained for adherent gram negative (blue) and positive (red) bacteria. Averages are given in Figure S5a.

(e–h) Example images of H&E stained duodenal section from Orai1$^{fl/fl}$ (e) and Orai1$^{-/-}$ mice maintained on LD (f) or SD diets (g). Inflammatory foci are marked by black arrows and collapsed villi are marked with turquoise arrows. (h) Shows the summary of inflammatory score for the three conditions.

(i–k) Bacterial infection of the spleen (i), liver (j) and pancreas (k).

(l) Intestinal permeability of the indicated mice.

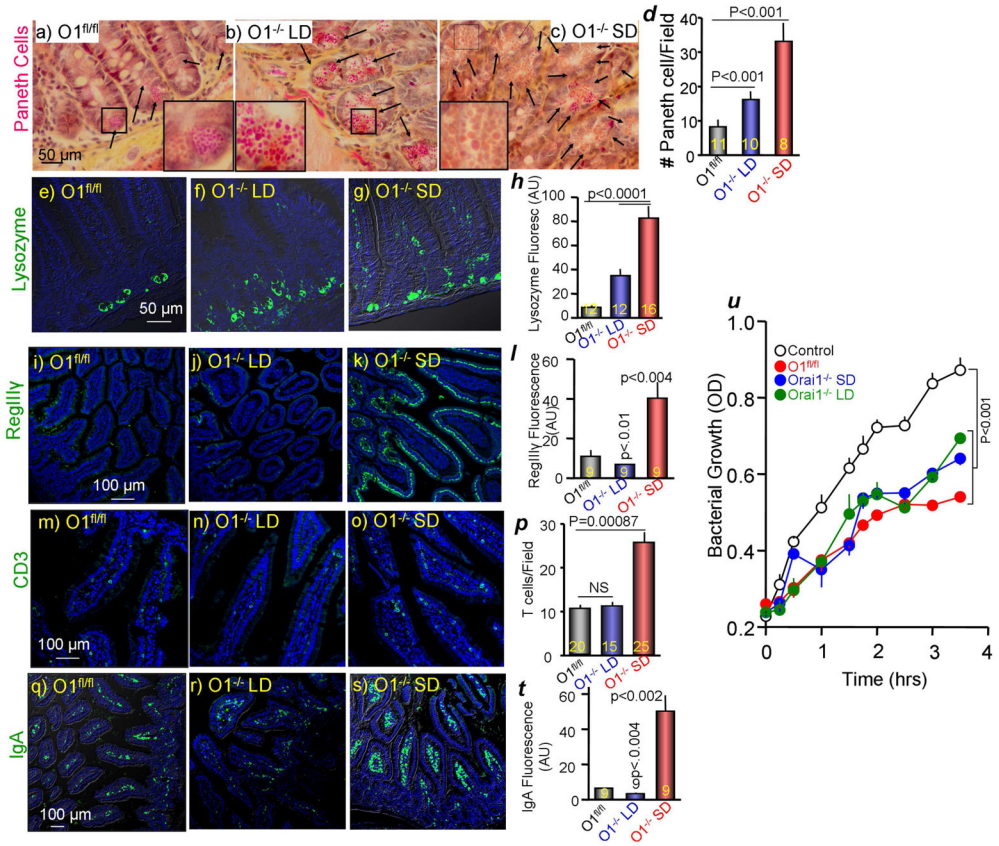

Figure 5. Analysis of intestinal innate immunity in Orai1$^{fl/fl}$ and Orai1$^{-/-}$ mice

(a–d) Phloxine B/tartrazine staining of intestinal sections obtained from Orai1$^{fl/fl}$ (a) and Orai1$^{-/-}$ mice maintained on liquid (b) or solid diet (c). (d) Shows the average number of Paneth cells/field analyzed in the indicated number of fields obtained from 3 mice in each line.

(e–h) Intestinal sections from 3 Orai1$^{fl/fl}$, 3 Orai1$^{-/-}$ mice on liquid diet and 4 Orai1$^{-/-}$ mice on solid diet were stained for lysozyme (green) and counterstained for DAPI (blue). (h) Shows the average lysozyme fluorescence in the indicated number of fields.

(i–l) Intestinal section from the indicated mice as in (e–h) were stained for RegIIIγ (green) and counterstained for DAPI (blue). (l) Shows the average RegIIIγ fluorescence.

(m–p) Intestinal section from the indicated mice as in (e–h) were stained for CD3 T cells (green) and counterstained for DAPI (blue). (p) Shows the average number of T cells/field analyzed in the indicated number of fields.

(q–t) Intestinal section from the indicated mice as in (e–h) were stained for IgA (green) and counterstained for DAPI (blue). (t) Shows the average IgA fluorescence in the indicated number of fields.

(u) Secreted duodenal antibacterial killing activity of Orai1$^{fl/fl}$ (red) and Orai1$^{-/-}$ mice maintained on liquid (green) or solid diet (blue). Results are mean±s.e.m of extracts obtained from 3 mice in each line. Deletion of pancreatic acinar Orai1 did not inhibit intestinal antibacterial secretion and killing.

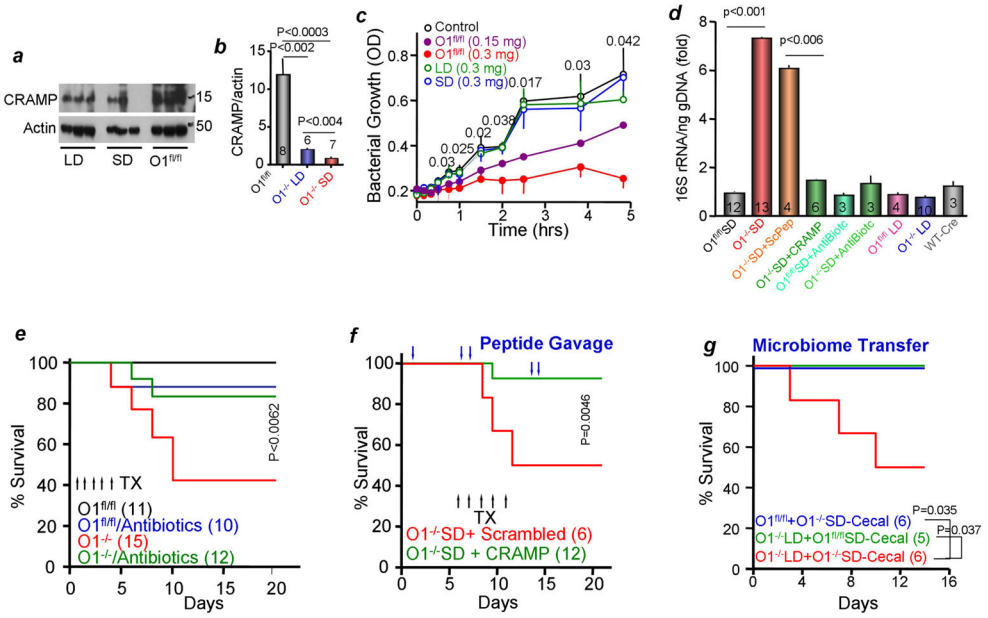

Figure 6. Pancreatic bacterial killing role in the gut microbiome

(a, b) Pancreatic extracts from Orai1$^{fl/fl}$ and Orai1$^{-/-}$ mice maintained on liquid or solid diets were analyzed for total CRAMP. Shown are sample blots and the average from the indicated number of mice is given in the columns.

(c) Secreted antibacterial killing activity by Orai1$^{fl/fl}$ and Orai1$^{-/-}$ acinar cells stimulated with 100 pM CCK8 is tested as inhibition of E. coli growth. The results are mean±s.e.m of extracts obtained from 3 mice in each line.

(d) Cecal 16S rRNA extracted from the indicated number of mice that were treated with CRAMP or scrambled peptides or antibiotics and maintained on LD or SD was measured by qPCR. Results are expressed as mean±s.e.m.

(e) Survival of mice untreated or treated with wide-spectrum antibiotics for one week before and during the experiment provided in drinking water. TX, tamoxifen

(f) Survival of Orai1$^{-/-}$ SD mice after gavage at the time indicated by the blue arrows with 100 μg CRAMP peptide dissolved in 200 μl PBS. Control mice were gavaged with scrambled peptide.

(g) Microbiome transplant was accomplished by gavaging Orai1$^{fl/fl}$ (blue) and Orai1$^{-/-}$ mice maintained on liquid diet (red) with cecal bacteria from Orai1$^{-/-}$ mice maintained on solid diet. As an additional control, Orai1$^{-/-}$ mice maintained on liquid diet were gavaged with cecal bacteria from Orai1$^{fl/fl}$ mice (green).

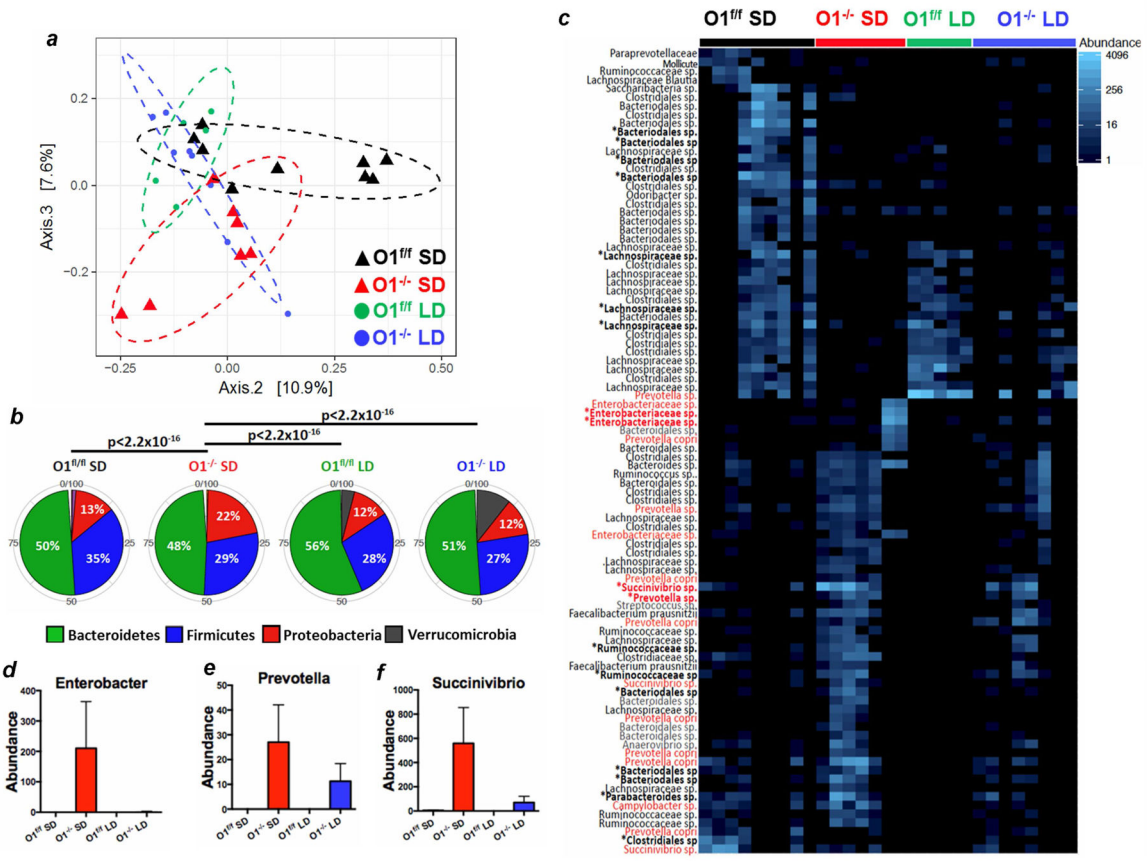

Figure 7. Analysis of the microbiome in Orai1$^{fl/fl}$ and Orai1$^{-/-}$ mice

(a) PCoA analysis in Orai1$^{fl/fl}$ mice maintained on solid diet (black), Orai1$^{fl/fl}$ mice maintained on liquid diet (green), Orai1$^{-/-}$ mice maintained on solid diet (red) and Orai1$^{-/-}$ mice maintained on liquid diet (blue). Increased distance between data points represents less similarity between overall taxonomic profiles

(b) The 5 most abundant phyla from each group of mice are shown. Proteobacteria are significantly enriched in the Orai1$^{-/-}$ mice on solid diet relative to the other groups.

(c) OTUs with differential expression between Orai1$^{-/-}$ mice and Orai1$^{fl/f}$ mice are shown. Asterisks denote OTUs with FDR-corrected p <0.05. Red denotes pathogenic strains.

(d–f) Differences in mean count for several pathogenic OTUs with FDR-corrected p<0.05 are shown between the four groups of mice.